NOAA Technical Report ERL 334-WPL 41

U.S. DEPARTMENT OF COMMERCE
NATIONAL OCEANIC AND ATMOSPHERIC ADMINISTRATION
Environmental Research Laboratories

Analysis of an All-Weather System for Wind Sounding up to 15 km Altitude

R. B. CHADWICK

E. E. GOSSARD

R. G. STRAUCH

BOULDER, COLO.
JUNE 1975

U.S. DEPARTMENT OF COMMERCE
Rogers C. B. Morton, Secretary

NATIONAL OCEANIC AND ATMOSPHERIC ADMINISTRATION
Robert M. White, Administrator
ENVIRONMENTAL RESEARCH LABORATORIES
Wilmot N. Hess, Director

NOAA TECHNICAL REPORT ERL 334-WPL 41

Analysis of an All-Weather System for Wind Sounding up to 15 km Altitude

R. B. CHADWICK
E. E. GOSSARD
R. G. STRAUCH

BOULDER, COLO.
June 1975

For sale by the Superintendent of Documents, U. S. Government Printing Office, Washington, D. C. 20402

DISCLAIMER

The NOAA Environmental Research Laboratories do not approve, recommend, or endorse any proprietary product or proprietary material mentioned in this publication. No reference shall be made to the NOAA Environmental Research Laboratories, or to this publication furnished by the NOAA Environmental Research Laboratories, in any advertising or sales promotion which would indicate or imply that the NOAA Environmental Research Laboratories approve, recommend, or endorse any proprietary product or proprietary material mentioned herein, or which has as its purpose an intent to cause directly or indirectly the advertised product to be used or purchased because of this NOAA Environmental Research Laboratories publication.

TABLE OF CONTENTS

ANALYSIS OF AN ALL-WEATHER SYSTEM FOR WIND SOUNDING UP TO 15 KM ALTITUDE

R. B. Chadwick, E. E. Gossard, and R. G. Strauch

Forward-scatter radio paths are analyzed as a means of remotely measuring winds to high altitudes. The propagation problem is formulated and pertinent equations are derived. A ranging technique using pseudo-noise modulation to measure the altitude of the scattering volume is described and several possible geometries and configurations are discussed. A sample design is suggested and the performance to be expected is calculated for that design. A rough estimate is given of the equipment cost for a nationwide system capable of routinely measuring winds up to 15 km.

1. INTRODUCTION

It is well known that accurate weather prediction depends on good observations of the winds aloft. Present rawinsonde balloon soundings are made every 12 hours at approximately 75 sites in the continental United States. Unfortunately this frequency of sounding is barely adequate to describe the very large scale, slowly changing features in the wind patterns, and even this sounding density is very costly in both manpower and materials. Halving the time interval between rawinsonde balloon soundings would double the material cost and almost double the manpower cost. As an alternative, an electromagnetic remote sensing system could monitor almost continuously the winds up to about 15 km in virtually all weather conditions.

Such a wind sounding system would use the forward scatter of electromagnetic waves by turbulence-induced fluctuations in the refractive index of the atmosphere. This phenomenon, commonly described as troposcatter, has been used for two decades in civilian and military communication systems. The systems have proved to be very reliable when properly engineered. The reliability of troposcatter communication systems can perhaps be extrapolated to wind sounding systems since these systems can operate with a much smaller signal-to-noise ratio than communication systems. Thus, it is clear that forward-scatter wind sounding should be investigated further.

A troposcatter system is, essentially, a sensitive bistatic radar whose transmitter and receiver are separated by 150 to 500 km. In such an arrangement the antennas point almost directly toward each other at a small grazing angle (a few degrees). Their beams intersect near

midpath forming a "common volume." The transmitted signal is received after it has been scattered from small-scale refractive index fluctuations in the common volume. If the scatterers are moving with a prevailing wind in the volume, a Doppler shift in frequency is introduced by the component of wind across the baseline of the system, and this is easily measured by coherent processing of the received signal. Vertical winds also contribute to the Doppler frequency shift, but the vertical wind contribution will usually be negligible compared with the horizontal wind and will average out over a period of time.

Several recent experiments using troposcatter systems have demonstrated the feasibility of using them for wind sounding. A wind sounding capability with the RAKE communication system was demonstrated by the University of Wisconsin and reported by Birkemeier et al. (1968, 1969) and Barrow et al. (1969). Their system was not designed as a wind sounding system so their center frequency was approximately 900 MHz rather than the 9 GHz we propose for measuring winds. Using the University of Wisconsin results, Atlas (1969) and Atlas et al. (1968) argued the feasibility of measuring winds aloft using forward scatter techniques and proposed a system by which wind measurements could be accomplished. More recently, Lammers and Olsen (1973) used an unmodulated 16 GHz system and demonstrated the capability of measuring winds to a height of about 15 km at even these short wavelengths. Each of these experimental systems for wind measuring performed very well, demonstrating the reliability of the forward scatter concept. In addition, the Bell Telephone Laboratories operated, for many months, a system whose common volume was at a height of 6 to 7 km, and at all times the signal was at a level where wind measurements could have been made.

By analyzing forward-scatter propagation and deriving the pertinent equations, we can calculate expected transmission loss for a particular wind sounding system. This allows us to calculate trade-offs in parameters such as antenna size, transmitter and receiver separation, transmitted power, etc., to achieve satisfactory performance at a reasonable cost. Application of the theory of bistatic ranging allows calculation of height resolution and output signal-to-noise ratios. This allows system performance to be predicted prior to setting up an experimental system. Using available technology, we believe that an operational wind sounding system can be realized that would provide nearly continuous and instantaneous estimates of winds up to tropopause heights.

2. FORWARD SCATTER PROPAGATION ANALYZED

2.1 Background

Our derivation of the forward scatter equations is based on that of Booker and Gordon (1950) in which they described atmospheric turbulence in terms of a spatial covariance function. Villars and Weisskopf (1955)

pointed out the relative simplicity of the formulation if the turbulence spectrum is used instead. The rise in popularity of the "structure function" represents a partial return to the use of the spatial covariance. In what follows we develop the relationships in terms of the spectrum, structure function, and reflectivity.

Consider a small element of a scattering volume common to both the transmitter beam and the receiver beam at which the incident electric field is

$$E_i \, e^{i\left(\omega t - \underset{\sim}{k}_i \cdot \underset{\sim}{r}_i\right)} ,$$

where

$$k_i = \frac{2\pi}{\lambda_e} ,$$

and λ_e is wavelength of the electromagnetic wave. Under the action of the electric field the small element (if dielectric) becomes polarized. If the element of volume, dV, has its dielectric perturbed by the amount $\delta\varepsilon$ above the unperturbed value ε_o, it behaves as a dipole of moment

$$M = E_i \, e^{i\left(\omega t - \underset{\sim}{k}_i \cdot \underset{\sim}{r}_i\right)} \delta\varepsilon \, dV .$$

At some (much greater than λ_e) range, $\underset{\sim}{r}_s$, from the scattering element, in the direction of the vector wavenumber $\underset{\sim}{k}_s$, the radiation from the dipole will be

$$E = A \, k_s^2 \sin\chi$$

where A, the Hertzian potential at the receiver, is given by

$$A = \frac{M}{4\pi \, \varepsilon_o \, r_s} \, e^{-i \underset{\sim}{k}_s \cdot \underset{\sim}{r}_s}$$

and χ is the angle between $\underset{\sim}{k}_s$ and the direction of polarization of E_i.

Therefore

$$E = \frac{e}{r_s} e^{-i \underset{\sim}{k}_s \cdot \underset{\sim}{r}_s} k_s^2 \frac{E_i}{4\pi} e^{i\left(\omega t - \underset{\sim}{k}_i \cdot \underset{\sim}{r}_i\right)} \frac{\delta\varepsilon}{\varepsilon_o} dV \sin\chi \qquad (1)$$

Assuming that the single scattering approximation is valid, and that the transmitter and receiver are so far from the scattering volume dV that $\underset{\sim}{r}_i$ and $\underset{\sim}{k}_s$ are nearly independent of position within the volume, dV, we can write

$$\underset{\sim}{k}_i \cdot \underset{\sim}{r}_i + \underset{\sim}{k}_s \cdot \underset{\sim}{r}_s = \underset{\sim}{k}_s \cdot \left(\underset{\sim}{r}_s + \underset{\sim}{r}_i\right) + \left(\underset{\sim}{k}_i - \underset{\sim}{k}_s\right) \cdot \underset{\sim}{r}_i$$

so, letting $\underset{\sim}{r}_s + \underset{\sim}{r}_i = \underset{\sim}{R}$, as in figure 1,

$$E = \frac{E_i}{2\pi} \sin\chi \; e^{i\left(\omega t - \underset{\sim}{k}_s \cdot \underset{\sim}{R}\right)} \frac{k_s^2}{r_s} \delta n \; e^{-i \underset{\sim}{K} \cdot \underset{\sim}{r}_i} dV \qquad (2)$$

where we have used the fact that $\delta\varepsilon/\varepsilon_o \simeq 2\,\delta n$, where n is refractive index, and where

$$|K| = \left|\underset{\sim}{k}_i - \underset{\sim}{k}_s\right| = 2k \sin\frac{\theta}{2} = 2\left(\frac{2\pi}{\lambda_e}\right) \sin\frac{\theta}{2}$$

From now on sine χ is omitted since it is very nearly unity ($\chi \simeq 90°$) and the r-f factor is omitted since the signal complex envelope is the factor of interest. Then, dropping subscripts on r, (2) can be written

$$E_s = \frac{E_i}{2\pi} \frac{k^2}{r} A(K) \quad ,$$

where

$$A(K) = \int_V \delta n \; e^{-i \underset{\sim}{K} \cdot \underset{\sim}{r}} dV \quad ,$$

thus retaining a general form for the spectrum of scatterers. The scattered power density is then

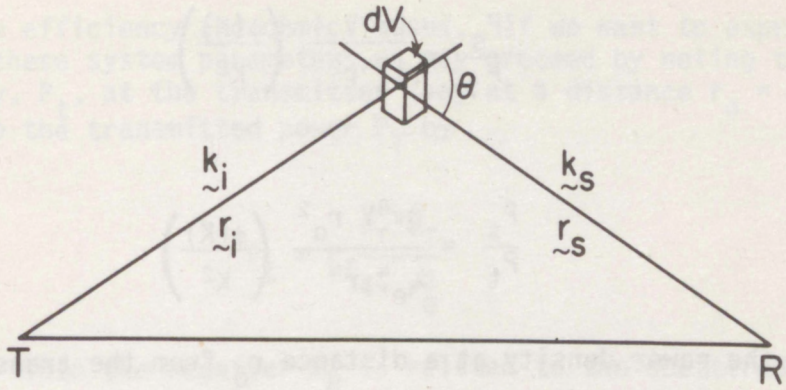

Figure 1. Scattering geometry for incremental volume (dV).

$$P_s \sim E_s\, E_s^* = \frac{E_i\, E_i}{(2\pi)^2} \frac{1}{r^2} \left(\frac{2\pi}{\lambda_e}\right)^4 A(\underset{\sim}{K})\, A^*(\underset{\sim}{K}) \quad .$$

If the scattering entities are homogeneously distributed through the volume V, it is convenient to define the quantity

$$F(\underset{\sim}{K}) = V^{-1} \frac{1}{8\pi^3} A(\underset{\sim}{K})\, A^*(\underset{\sim}{K})$$

which is the spectrum of refractive index $n(\underset{\sim}{r})$ in the sense that

$$F(K) = \frac{1}{8\pi^3} \int \delta n(\underset{\sim}{r'})\, \delta n(\underset{\sim}{r'}+\underset{\sim}{r})\, e^{-i\, \underset{\sim}{K} \cdot \underset{\sim}{r}}\, d^3r.$$

Then

$$\frac{P_s}{P_i} = \frac{8\pi^3}{(2\pi)^2} \left(\frac{2\pi}{\lambda_e}\right)^4 \frac{1}{r^2}\, V\, F(\underset{\sim}{K})$$

where P_i is the incident power density and P_s is the scattered power density. If we now make the important assumption that the inhomogeneities are isotropic, the spectrum in scalar K is just $\phi(K) = 4\pi K^2\, F(\underset{\sim}{K})$ so that

$$\frac{P_s}{P_i} = \frac{8\pi^4 V}{\lambda_e^4 r^2} \left(\frac{\phi(K)}{K^2}\right)$$

or

$$\frac{P_s}{P_t} = \frac{8\pi^4 V\ r_o^2}{\lambda_e^4\ r^4} \left(\frac{\phi(K)}{K^2}\right)$$

where P_t is the power density at a distance r_o from the transmitter. We have assumed symmetry, i.e., $r_s = r_i = r$, and dropped the subscripts.

Therefore, the appropriate expression for the scattered power density at the receiver is

$$\frac{P_s}{P_t} = r_o^2 \frac{8\pi^4}{\lambda_e^4} \frac{V}{r^4} \frac{\phi(K)}{K^2} = \frac{\eta V}{4\pi} \frac{r_o^2}{r^4} \qquad (3)$$

where η is the radar reflectivity and ηV is the scattering cross section. Here η has been defined as $2\pi\ (2\pi/\lambda_e)^4\ \phi(K)/K^2$ in agreement with Ottersten (1969). If the two antenna beamwidths, α_T, α_R, are very narrow (i.e., $\alpha < (2/3)\ \theta$), the common volume intercepted by the transmitting and receiving antennas is given by (see Booker and deBettencourt, 1955)

$$V = \frac{r^3\ \alpha^3}{4\ \theta} \ ,$$

where the intersecting beams have been treated as two long, thin cylinders. Again we have dropped the subscripts because of symmetry. On substituting into (3)

$$\frac{P_s}{P_t} = r_o^2 \frac{8\pi^4}{\lambda_e^4} \frac{\alpha^3}{4r\theta} \frac{\phi(K)}{K^2} \frac{r_o^2\ \eta\alpha^3}{16\pi r\theta} \ . \qquad (4)$$

This is the transmission loss equation for a narrow beam forward-scatter path.

So far, the analysis has not concerned radar system parameters such as transmitted power P_T and gain G_T, effective receiving antenna aperture A_e, and efficiency factors β_T, β_R. These efficiency factors involve

both aperture efficiency and ohmic losses. If we want to express (4) in terms of these system parameters we may proceed by noting that the power density, P_t, at the transmitter (say at a distance r_o = 1 meter) is related to the transmitted power P_T by

$$P_t = P_T \frac{\beta_T \, G_T}{4\pi \, r_o^2}$$

and the power into the receiver P_R is related to the scattered power density, P_s, at the receiving antenna by

$$P_R = P_s \, A_e \, \beta_R = P_s \, \frac{\lambda_e^2 \, G_R \, \beta_R}{4\pi}$$

where the effective aperture is given by $A_e = \lambda_e^2 \, G_R/4\pi$. So

$$\frac{P_R}{P_T} = \frac{P_s}{P_t} \left(\frac{\lambda_e^2 \, G_R \, G_T \, \beta_R \, \beta_T}{16\pi^2 \, r_o^2} \right) \tag{5}$$

and, if we approximate the antenna performance by $G_R = G_T \simeq 16/\alpha^2$ (where α is the width of a rectangular beam in radians), (4) becomes

$$\frac{P_R}{P_T} = \beta_R \, \beta_T \, \frac{\lambda_e^2 \, \eta}{\pi^3 \alpha r \theta} \, . \tag{5a}$$

The reflectivity η, in units of $(m)^{-1}$, is related to the refractive index spectrum $\phi(K)$ by

$$\eta = 2\pi \left(\frac{2\pi}{\lambda_e} \right)^4 \frac{\phi(K)}{K^2}$$

and, if a Kolmogoroff spectrum is chosen, the spectrum $\phi(K)$ can be expressed in terms of the structure constant C_n^2 (see Ottersten, 1969) so that

$$\eta \simeq \frac{\pi}{2}\left(\frac{2\pi}{\lambda_e}\right)^4 C_n^2 K^{-11/3} \qquad (6)$$

where C_n is defined by the structure function

$$D(\ell) = C_n^2 \ell^{2/3}$$

and where D is the variance of the difference in refractive index at two sensors separated by the distance ℓ.

Since $K = 2\left(\frac{2\pi}{\lambda_e}\right)\sin\frac{\theta}{2}$, an alternative form for η is

$$\eta = \frac{\pi}{32}\left(\frac{4\pi}{\lambda_e}\right)^{1/3} C_n^2 \left(\sin\frac{\theta}{2}\right)^{-11/3}$$

so when $\theta/2$ is a small angle, (5a) becomes

$$\frac{P_R}{P_T} = 2\,\beta_R\,\beta_T\left(\frac{2\pi}{\lambda_e}\right)^{-5/3}\left(\frac{C_n^2}{\alpha r}\right)\theta^{-14/3} \quad . \qquad (7)$$

Returning to (5) we can also retain the gains explicitly, if desired, and write

$$\frac{P_R}{P_T} = \beta_R\,\beta_T\,G_R\,G_T\left(\frac{1}{512}\right)\left(\frac{4\pi}{\lambda_e}\right)^{-5/3}\frac{\alpha^3}{r}\frac{(\sin\theta/2)^{-11/3}}{\theta}C_n^2 \qquad (8)$$

so $\frac{P_R}{P_T} = \beta_R\,\beta_T\,G_R\,G_T\,(L)^{-1}$ can be used to define a basic transmission loss L, which is effectively the path loss between the antennas. This loss depends on the antenna sizes, on the value of C_n^2, and on the scattering angle.

2.2 Forward-Scatter Link Geometry

The atmosphere is slightly refractive to microwaves so rays are not truly straight lines. Instead they bend downward. Without unduly

complicating the geometrical calculations, we can take this effect into account by changing the effective earth radius. In what follows we assume it to be 4/3 its true value, so a = 8494 km.

Consider the quantities defined in figure 2 and remember that the angles are actually very small and that all lengths associated with the radio path are very small compared with the effective Earth radius a. Then

$$a^2 + r^2 = (a + h)^2 \simeq a^2 + 2\,ah$$

so

$$h \simeq \frac{r^2}{2a} = \frac{1}{4} r\,\theta \qquad \text{and} \qquad r = \sqrt{2\,ah}$$

since $r/a \simeq \theta/2$. Furthermore

$$\frac{h + h'}{r} = \sin\frac{\theta}{2} \simeq \frac{\theta}{2} \quad ,$$

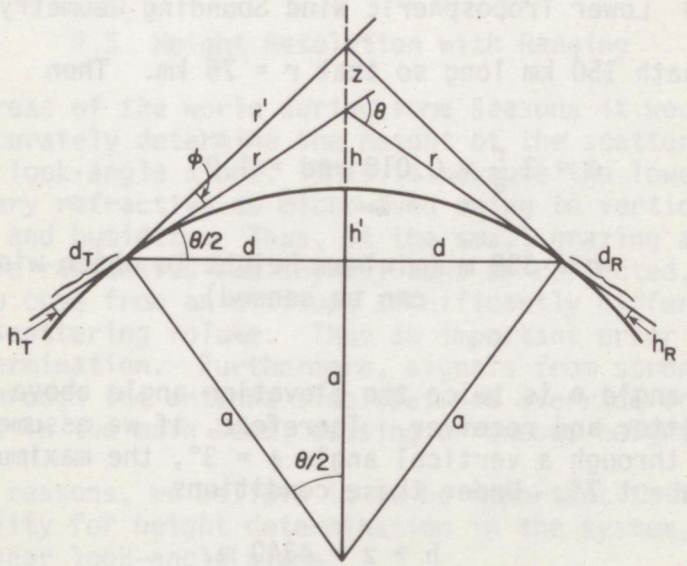

Figure 2. Forward scatter geometry.

so

$$h + h' \simeq \frac{1}{2} r\,\theta \qquad \text{and} \qquad h \simeq h' \quad .$$

Also

$$\sin\left(\frac{\theta}{2} + \phi\right) = \frac{h + h' + z}{r'} \simeq \frac{\theta}{2} + \phi$$

so

$$\frac{\frac{1}{2} r\,\theta + z}{r'} \simeq \frac{\theta}{2} + \phi$$

and

$$z \simeq \phi\, r \quad .$$

Raising the height of the transmitting and receiving antenna effectively decreases r for the same total path length, thus decreasing h and θ. If the antenna is raised to a height h_R, then

$$d_R \simeq \sqrt{2\, a\, h_R} \quad .$$

2.3 Lower Tropospheric Wind Sounding Geometry

Choose a path 150 km long so that r = 75 km. Then

$$\theta = 2\,\frac{r}{a} = 0.018 \text{ rad} = 1.0°$$

and

$$h = 338 \text{ m (minimum height to which winds can be sensed).}$$

The scattering angle θ is twice the elevation angle above the cord between transmitter and receiver. Therefore, if we assume that the beam is to be swept through a vertical angle $\phi = 3°$, the maximum scattering angle will be about 7°. Under these conditions

$$h + z = 4340 \text{ m.}$$

A 20-ft diameter antenna with a beamwidth of 0.44° would provide a 600-m height resolution (seven levels) within this height range.

2.4 Upper Tropospheric Wind Sounding Geometry

Choose a path 540 km long so that r = 270 km. Then

$$\theta = 2\frac{r}{a} = 0.064 = 3.6°$$

and

h = 4320 m (minimum height to which winds can be sensed).

We will assume the beam is to be swept vertically through $\phi = 2.5°$, so the maximum scattering angle will be 8.8°, approximately the same as the path used by Lammers and Olsen (1973). Under these conditions $z \simeq 12$ km, so

$$h + z = 16{,}300 \text{ m}$$

is the maximum height to which winds can be sensed.

The resolution attainable when there is no ranging capability is determined by the beamwidth and the radial distance to the scattering volume. A 60-ft diameter antenna with a beamwidth of 0.13° would provide a height resolution of 600 m, or 15 levels between 5700 m and 15,200 m elevation. A 30-ft diameter antenna would provide half as many levels with a resolution of about 1200 m. Eq. (7) shows that the received power would then be halved with a resulting loss of 3 dB.

2.5 Height Resolution with Ranging

In some areas of the world during some seasons it would not be possible to accurately determine the height of the scattering volume from the radar look-angle alone. This is because the lower atmosphere is sometimes very refractive to microwaves owing to vertical gradients of temperature and humidity. Thus, at the small grazing angles used in this system, the radiowaves are sharply bent or reflected, and the signal would appear to come from an altitude significantly different from that of the actual scattering volume. Thus an important error might occur in the height determination. Furthermore, signals from strong scatterers might arrive through the antenna sidelobes and override or compete with weak scatterers in the main beam, causing erroneous heights to be inferred.

For these reasons, we believe it to be important to include a ranging capability for height determination in the system, rather than to depend on radar look-angle alone.

The scattering geometry is shown schematically in figure 3. The surfaces of constant range are ellipsoids of revolution whose foci are

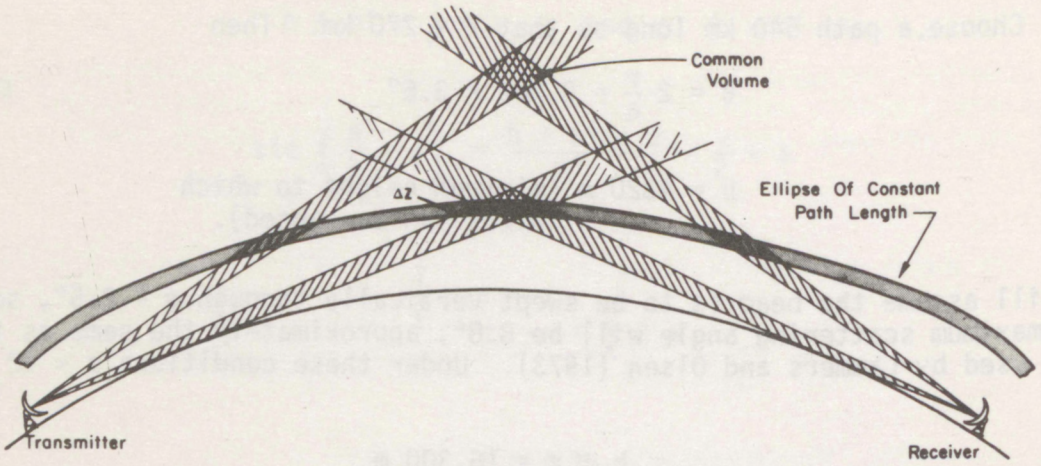

Figure 3. Vertical cross section (schematic) of forward-scatter Doppler wind profiler (approximately 2° off great circle path.)

the transmitter and receiver. A height (or path length) resolution increment is indicated by the shaded thickness of the ellipsoid shown. Define $z' = h + h' + z$ so that

$$r = \sqrt{d^2 + z'^2}$$

and

$$\tau = \frac{2r}{c} \quad \text{where} \quad \tau = \text{total time delay.}$$

Therefore

$$\tau = \frac{2}{c}\left(d^2 + z'^2\right)^{1/2} ,$$

so

$$\frac{d\tau}{dz} = \frac{2}{c}\left(d^2 + z'^2\right)^{-1/2} z'$$

and

$$\Delta\tau = \frac{2z'}{c\sqrt{d^2 + z'^2}}\ \Delta z ,$$

where Δz is height resolution and $\Delta\tau$ is time resolution. So

$$\Delta z \gtrsim \frac{cd}{2z'} \Delta\tau \quad .$$

But

$$\tan \frac{\theta}{2} = \frac{z'}{d} \simeq \frac{\theta}{2} \text{ (rad)} \simeq \frac{\pi}{180°} \frac{\theta°}{2}$$

where $\theta°$ is scattering angle in degrees. Therefore

$$\Delta z \simeq c \frac{180}{\pi} \frac{\Delta\tau}{\theta} \quad .$$

For purposes of illustration, we assume $\Delta\tau = 10^{-7}$ sec and $\frac{\theta}{2} = 1°$; $\frac{\Delta\tau}{\theta} = 0.5 \times 10^{-7}$ so at the bottom of the scattering volume where $z' = h + h'$, the height resolution is

$$\Delta z = \frac{3 \times 10}{2} \frac{180}{\pi} = 860 \text{ m} \quad .$$

However for a scattering angle of 10°, Δz = 170 m. Thus the ranging capability of a system improves at higher altitude (and on longer paths) for which the scattering angle is fairly large. If the resolution of a 30-ft diameter antenna is adequate for meteorological purposes on the long path, only a 0.7 μsec modulation would be required for a matching height ranging capability.

There is a trade-off between resolution and signal-to-noise ratio since better resolution reduces the spatial integration. However, as discussed below, the degradation in signal-to-noise ratio is significant only at the higher altitudes and can be easily corrected by changing the clock rate.

2.6 Transmission Loss vs. Elevation Angle

Eq. (7) or (8) can be used in the calculation of received power for beam-weighted volume. The value C_n^2 in the atmosphere has been variously measured and estimated as ranging from 10^{-15} to 10^{-13} $m^{-1/3}$, so we have calculated curves of transmission loss L vs. elevation angle (figs. 4 and 5) for these three values of C_n^2. We can calculate the received power for a known transmitted power and known antenna gains and compare it with the minimum detectable signal. The curves in figures 4 and 5 are for a 3-cm radar system assuming 60-ft and 30-ft diameter antennas on the long path (540 km) in figure 4 and a 20-ft diameter antenna on the short path (150 km) in figure 5. The respective gains are 65 dB, 59 dB, and 54 dB.

Similar calculations for the path used by Lammers and Olsen (1973) were carried out with

λ_e = 1.9 cm

2r = 498 km

G_T = 59.3 dB

G_R = 60.1 dB

P_T = 1.3 kW

Min. detect. sig. = - 145 dBm

α= 0.00262 rad = 0.15°.

The plot of L vs. ϕ is shown in figure 6. For L = -295 and the antenna gains above, we find a signal of -106 dBm or -116 dBm or -126 dBm depending on our choice of C_n^2. Thus the calculated signal is about 30 dB above the minimum, in satisfactory agreement with the fields measured by Lammers and Olsen shown in figure 7 and with received power cumulative frequency distributions shown in figure 8. Figure 7 shows received power as a function of the location of the scattering volume along the path. It was obtained by moving the antennas in a synchronized manner and recording the received power. From figure 8, the scattered field from an elevation angle of 2° (about 15 km elevation) should be detectable somewhat more than 50 percent of the time, in agreement with our theoretical calculation. However, it should be remembered that we used a two order of magnitude range for C_n^2, chosen on the basis of measured C_n^2 values in the lower atmosphere. Confirmation of these values in the upper atmosphere is provided by the clear-air backscatter from the upper troposphere detected by the Wallops Island 10-cm radar of NASA.

3. MODULATION TECHNIQUES

If a system transmits a narrow-band CW signal, the output signal-to-noise ratio can be relatively high, so larger scattering angles can be tolerated than for broad-band systems. However, if a system has ranging capability, the height resolution and height accuracy of the sounder are very significantly improved, especially at the higher angles. The system also becomes more immune to narrow-band interference. This reduces the problem of siting the receiver in an electromagnetically noisy area. In addition, when looking at higher angles, the ranging capability removes the problem of signals from the sidelobes at lower angles.

There are several different approaches to modulation of the transmitted signal to perform the ranging. One obvious approach is to

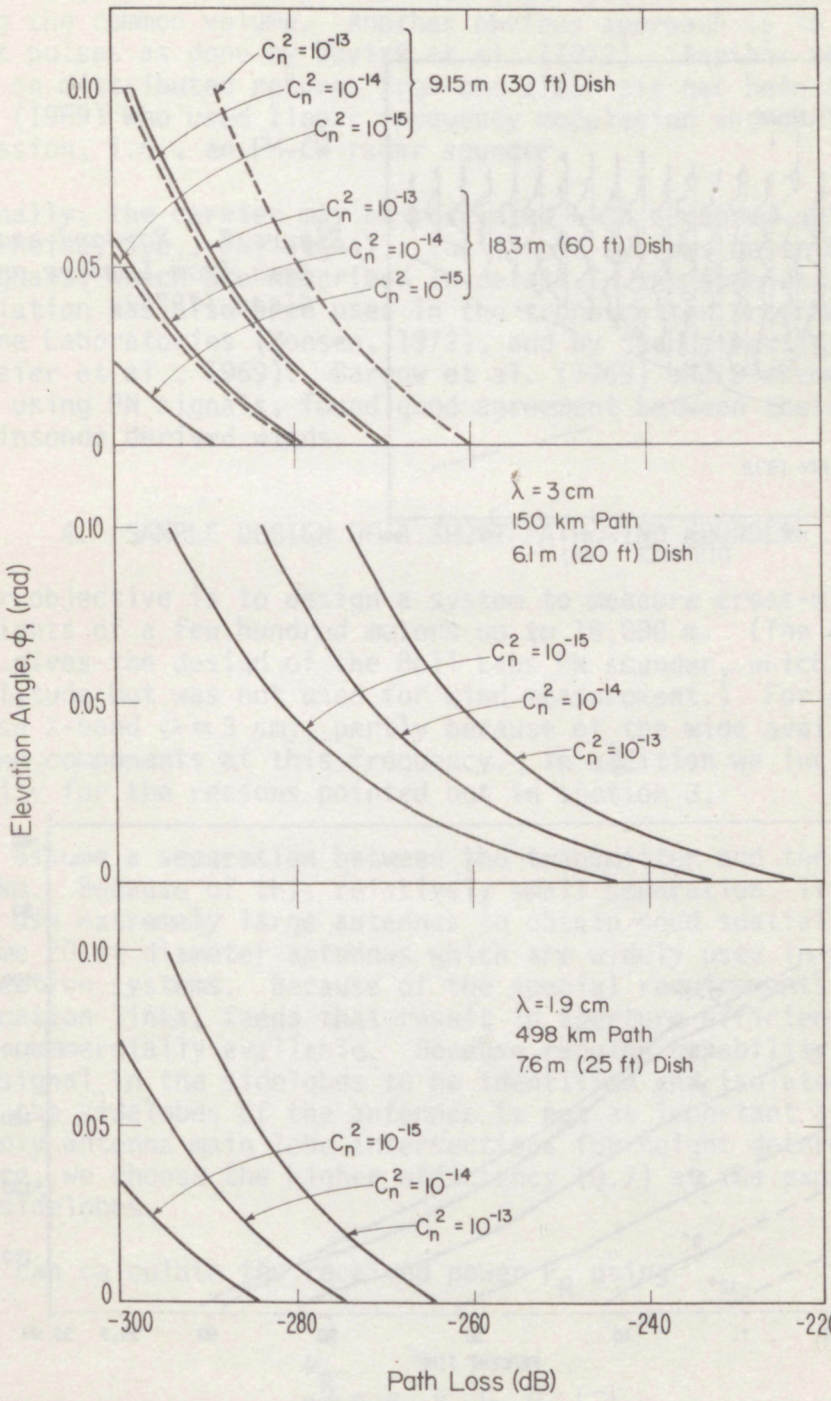

Figure 4.

Figure 5.

Figure 6.

Figures 4, 5, and 6. Path loss, as defined in eq (8), vs. elevation or look angle. Figure 6 corresponds to the Lammers and Olsen (1973) path.

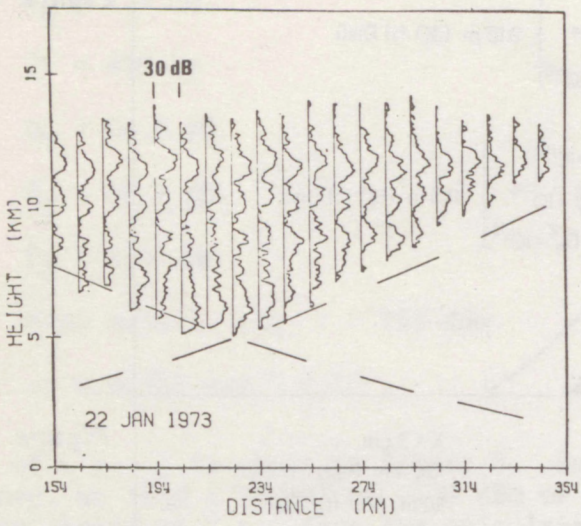

Figure 7. Forward-scatter data from Lammers and Olsen (1973).

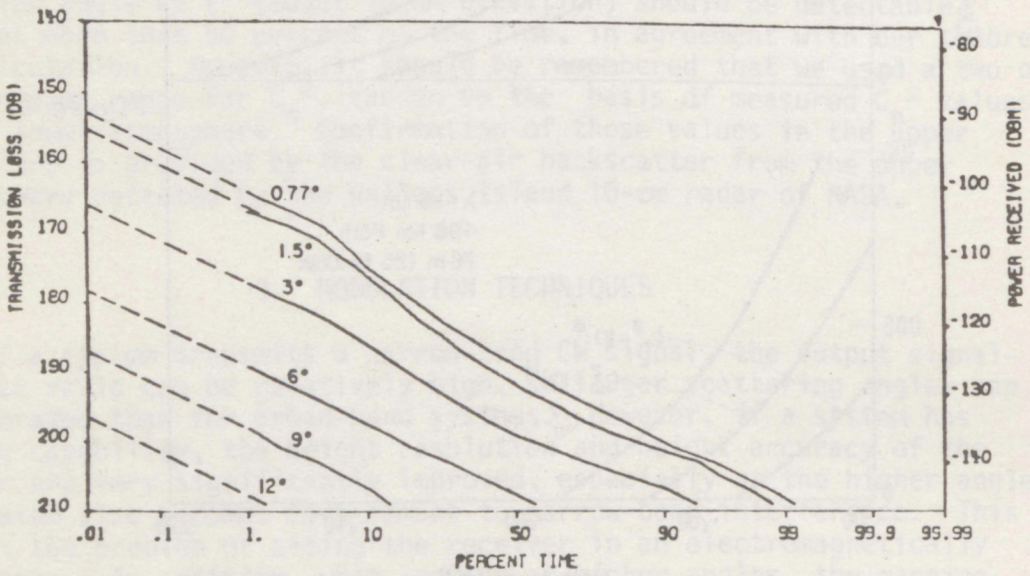

Figure 8. Received power distributions as a parameter of look angle.

use CW transmission and determine the range to the scattering volume (and its height) from the geometrical intersection of narrow beams bounding the common volume. Another obvious approach is to transmit coherent pulses as done by Doviak et al. (1972). Another technique for ranging on distributed returns from the clear air has been described by Richter (1969) who used linear frequency modulation and continuous wave transmission, i.e., an FM-CW radar sounder.

Finally, the carrier may be modulated with a random or pseudo-random (pseudo-noise, i.e., PN) signal. The sample systems described here use such signals, which are described in detail in the Appendix. This kind of modulation has also been used in the troposcatter program at Bell Telephone Laboratories (Monsen, 1972), and by the University of Wisconsin (Birkemeier et al., 1969). Barrow et al. (1969) and Birkemeier et al. (1969), using PN signals, found good agreement between their measurements and rawinsonde derived winds.

4. SAMPLE DESIGN OF A SHORT-PATH WIND SOUNDER

Our objective is to design a system to measure cross-wind velocities from heights of a few hundred meters up to 15,000 m. (The Appendix, Part D, gives the design of the Bell Labs PN sounder, which operated to 7 km altitude but was not used for wind measurement.) For our example we choose X-band ($\lambda \approx 3$ cm), partly because of the wide availability of parts and components at this frequency. In addition we include ranging capability for the reasons pointed out in section 3.

We assume a separation between the transmitter and the receiver of 150 km. Because of this relatively small separation, it is not necessary to use extremely large antennas to obtain good spatial resolution. We assume 20-ft diameter antennas which are widely used in satellite communication systems. Because of the special requirements of satellite communication links, feeds that result in aperture efficiences exceeding 0.7 are commercially available. Because ranging capability in the system allows signal in the sidelobes to be identified and isolated, suppression of the sidelobes of the antennas is not as important as in systems using only antenna main lobe intersections for height determination. Therefore, we choose the higher efficiency (0.7) at the expense of higher sidelobes.

We can calculate the received power P_R using

$$\frac{P_R}{P_T} = \beta_R \, \beta_T \, G_R \, G_T \, L^{-1}$$

where β is the aperture efficiency, L is the path loss computed previously, and G is the antenna gain given by

$$G = \frac{4\pi A}{\lambda^2} = \pi^2 \left(\frac{D}{\lambda}\right)^2 .$$

In this equation, A is the physical area and D is the diameter. So

$$\frac{P_R}{P_T} = 48 \left(\frac{D}{\lambda}\right)^2 L^{-1}$$

which can be handled more conveniently by expressing all quantities in decibels:

$$P_R \text{ (dBW)} = P_T \text{ (dBW)} + 16.8 \text{ dB} + 4\ D/\lambda \text{ (dB)} + L \text{ (dB)}$$

The positive sign on L in the above equation results from our definition of L as a negative quantity in figures 4, 5, and 6. A 20-ft antenna has a D/λ of 23 dB at X band, and if we specify a 1 kW (+30 dBW) klystron power amplifier, we obtain

$$P_R = 138.8 \text{ dBW} + L \text{ (dB)} .$$

Values of L for different angles and different C_n^2 are readily obtained from figures 4, 5, and 6.

Next we find the received noise power P_N given by

$$P_N = k\, T_{eff}\, B$$

where k is Boltzman's constant, T_{eff} is the effective noise temperature and B is the system bandwidth. Uncooled parametric amplifiers have a noise figure of 3.5 dB and this would result in a system noise figure of 500°K at X band. If we use PN modulation for ranging, and clock the PN code at 10 MHz, i.e., a bit time of 0.1 μs, the bandwidth B is 10^7 Hz. This leads to a receiver noise power of -131.5 dBW.

Now we can calculate the output signal-to-noise ratio using (A16) from the Appendix where M is time-bandwidth product of the signal, or the number of bits in the PN code,

$$SNR_o = 2M \frac{P_R}{P_N} .$$

Expressed in dB,

$$SNR_o = 273.3 \text{ dB} + L(\text{dB}) + M(\text{dB}).$$

This equation implies that by continuing to increase M, we can always increase the signal-to-noise ratio. While this may be true for zero velocity, it is not true when the received signal is Doppler shifted. A rule of thumb is that if T is the time length of the code and f_{max} is the maximum Doppler shift expected, then increasing T ceases to improve the signal-to-noise ratio when T f_{max} exceeds about 1/4. Birkemeier et al. (1969) show that the Doppler shift is $f = \frac{2V}{\lambda} \sin \phi_a$ where V is the cross-baseline wind velocity and ϕ_a is the azimuthal pointing angle measured from the baseline. For a maximum V of 100 m/s and an azimuthal pointing angle of 0.09 radians, $f_{max} \simeq$ 600 Hz so $T \lesssim 2 \times 10^{-4}$ and $M \lesssim 4170$. Therefore for V_{max} ϕ_a = 9, the maximum number of bits M in the code is 4095, which is provided by a 12-bit shift register and gives a processing gain of 36 dB.

The receiver output signal-to-noise ratio can now be found. Using M = 4095 or 36 dB, we find

$$SNR_o = 309.3 \text{ dB} + L \text{ (dB)} \quad .$$

The path loss L can be found from the graphs in figures 4, 5, and 6 and depends on two factors -- the structure constant C_n^2, and the vertical look angle ϕ which determines the altitude being probed. The structure constant generally ranges from 10^{-13} to 10^{-15}. We use a value of 10^{-14} and note that the loss (and the signal-to-noise ratio) can vary 10 dB in either direction. A vertical look angle of ϕ = 5.7° (see fig. 2) results in a maximum altitude of 7925 m and a path loss of - 278 dB. A look angle of 11.4° results in a maximum altitude of 15,425 m and a path loss of -292 dB. The output signal-to-noise ratio would still be +17 dB and if the C_n^2 value dropped to 10^{-15} (its lower value) the output signal-to-noise ratio would still be +7 dB. Our experience with the WPL dual-Doppler radar system indicates that useful velocity information can be obtained when the signal-to-noise ratio is in the range of 1 or 2 dB, so this design would allow for 3 or 4 dB degradation at the highest range with the smallest structure constant.

There are three types of signal-to-noise ratio degradation. The first type results because it is not possible to duplicate precisely the transmitted signal at the receiver. For situations where the signal is generated digitally, as in the PN sounder, the loss is generally small, i.e., of the order of 1 or 2 dB. If the signal is generated by analog means, the degradation can be much larger. For the FM-CW radar it is of the order of 10 dB.

The second type of signal-to-noise degradation results from reduction of the effective common volume due to ranging. This degradation can be neglected when the height resolution is poorer than 450 m. When the scattering is due to a thin layer rather than the entire volume, the sounder will be able to isolate the layer, and the signal is then

independent of the size of the common volume. If the signal-to-noise reduction is too large, an easy solution is to reduce the bandwidth of the transmitted signal, thus increasing the effective scattering volume while degrading the height resolution. The degradation would be acceptable since the resolution attainable at higher altitudes is significantly better than that needed for wind sounding.

The third type of signal-to-noise ratio degradation is that due to velocity dispersion of the target. To obtain the gain specified here, the return signal must lie in a single velocity resolution cell. The coherent integration of this system is the time duration of the PN code (0.4 ms) times the number of points Fourier transformed, and the Doppler frequency resolution is the reciprocal of this. This represents an allowable velocity dispersion of 1.2 m/s if there are 32 points in the Fourier transform. Experimental data from Barrow et al. (1969) show a maximum velocity dispersion of only 1 or 2 m/s. So this degradation can be neglected here.

The characteristics of our sample design are summarized in Table 1.

Table 1. Parameters of Short-Range Wind Sounding System.

Minimum sounding altitude	425 m
Maximum sounding altitude	15,425 m
Baseline separation	150 km
Wavelength	3 cm
Antenna diameter	20 ft
System effective temperature	500°K
PN code length	4095
Transmitted power	1 kW cw

The forward scatter wind sounding system has an unfortunate characteristic; the height resolution degrades with decreasing height. This means that the poorest resolution is obtained closest to the surface, where we would like it to be best. Figure 9 shows the height resolution as a function of the height for our sample system.

5. CONFIGURATIONS AND COSTS

It is not the intent of this report to present a complete cost analysis nor to explore the consequences of various trade-offs in system configuration. Such detailed analyses should be carried out after potential users have shown significant interest in the basic concepts.

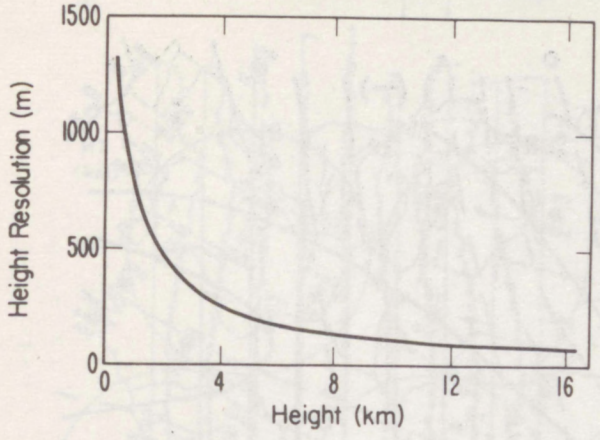

Figure 9. Height resolution as a function of height for sample wind-sounding system.

It is our purpose in this section to suggest a few possibilities in system configuration and to say a little about the cost of some major components. There are many additional costs such as site acquisition, training of personnel, and studies of the optimum reporting and use of the new data. Costs like these will often depend on such considerations as the extent to which present weather radar sites can be used for forward scatter terminals and whether personnel who now operate and maintain the weather radars can also operate and maintain the new equipment.

Throughout this report we are concerned with measuring the horizontal winds. This is possible with the system described here as, at the altitudes of interest, the vertical winds are negligible.

5.1 Upper Tropospheric Wind Sounding (Above 5 km Elevation)

5.1.1 Configuration

A possible configuration of transmitters and receivers for wind sounding the upper troposphere is shown schematically in figure 10. Eight transmitters and 32 receivers would replace the present GMD sounding system and essentially measure winds continuously above 5 km elevation for the continental U.S. The transmitters and receivers would have fixed 60-ft or 30-ft antennas (depending on the height resolution needed). Although fixed relative to the horizontal plane, the antennas would be designed to rotate (slowly), perhaps on circular steel tracks on the leveled ground. The 0.13° or 0.26° beams would be swept slowly through about 2° of vertical elevation angle. The transmitter antenna would point toward (about 2° off the great circle path) each of four receivers separated by 90° sequentially. A vertical sounding of the horizontal wind transverse to the radio path would be taken by each receiver as the beam of each was stepped upward in elevation in angular increments corresponding to the beamwidth of the antenna and the ranging resolution of the modulated transmission. Figure 10 also shows schematically the resulting wind field at perhaps the 100 mb height. Isotachs of east-west (solid curves) and north-south (dashed) curves have been drawn in

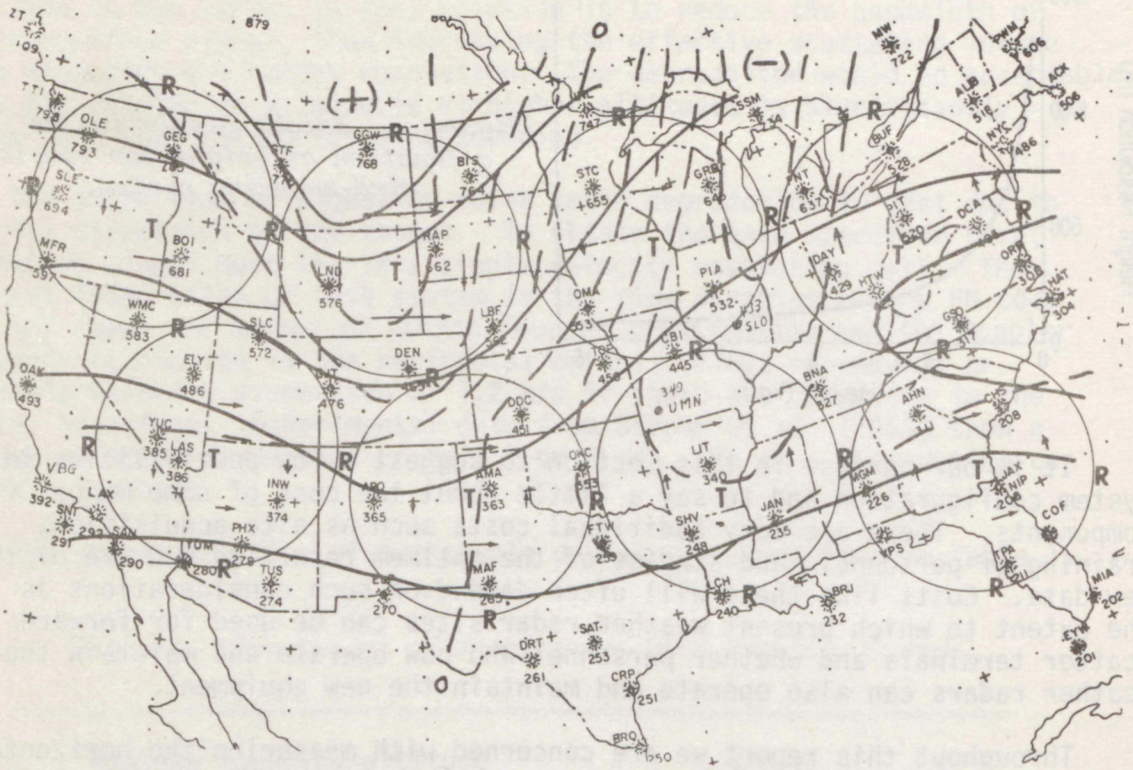

Figure 10. A configuration of 8 transmitters (T) and 22 receivers (R) for upper troposphere wind sounding. Solid lines are E-W isotachs; dashed lines are N-S isotachs.

accord with the transverse winds indicated by arrows at midpath. These winds are spatially averaged over a distance of about 200 km along the path, but the average is weighted toward the center of the path. A sample sounding taken over the Lammers and Olsen path is shown in figure 11.

5.1.2 Equipment Cost for System of 8 Transmitters and 22 Receivers

System:

γ = 3 cm

Power = 1 kW

Receiver noise temp = 500°

Pseudo-random noise code: 1023, 0.5 μs bits

Antenna: 60-ft or 30-ft dishes

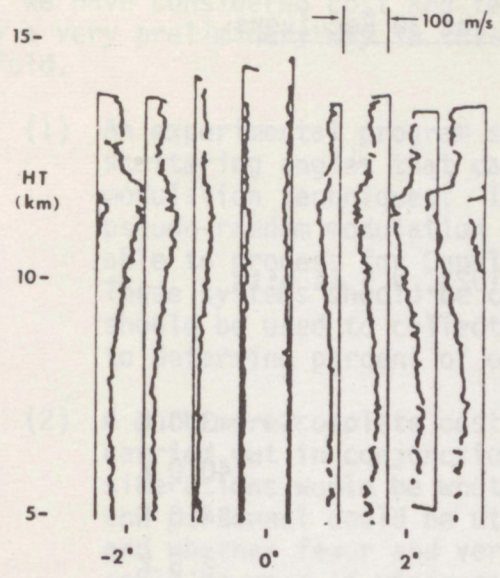

Figure 11. Winds measured with the Lammers and Olsen system between Boston and Ottawa. Lower scale is angle off the great circle path. Velocity scale (above) is given for sounding at an off-path angle of about 1.8. Note layer of strong shear at 12 km, and spatial uniformity of velocity patterns.

Equipment Costs:

Receiver pre-amp	$ 3.0 K	
30-ft antenna	60.0 K	
60-ft antenna	160.0 K	
Power amplifier (Klystron)	24.0 K	
Stable source (2 each)	2.5 K	
Signal processor (no computer)	5.0 K	
Upper atmospheric system total for 8 transmitters and 22 receivers	2,200.0 K	30-ft antennas
	5,200.0 K	60-ft antennas

5.2 Lower Tropospheric Wind Sounding (Below 5 km Elevation)

5.2.1 Configuration.

Simply placing a lower-power transmitter with a 20-ft dish 150 km from each of the receivers in the upper troposphere system would provide a grid mesh size of about 500 km. An additional receiver located 150 km away on a different azimuth would measure total wind near each of the R sites; two more receivers 150 km away from each of the T sites would provide wind velocity and direction at a total of 30 stations.

5.2.2 Cost of Adding 22 Transmitters and 30 Receivers.

System:

λ = 3 cm

Power = 1 kW

Receiver noise temp = 500°

Pseudo-random noise code: 1023, 0.5 μs bits

Antenna: 20-ft dish

Equipment Cost

Receiver pre-amp	$ 3.0 K
20-ft dish	40.0 K
Power amplifier (Klystron)	24.0 K
Stable source	2.5 K
Signal processor (no computer)	5.0 K
Total added cost of lower atmosphere system	2,900.0 K

5.2.3 An Alternative Configuration.

A configuration that provides orthogonal components of the wind at a single receiver site such as those designated by the R's in figure 10 is possible. Such a system would be more expensive since it would need two additional transmitters located 150 km from each R, or 44 additional transmitters, at a cost of approximately $3900 K. However, it is unquestionably attractive to have both wind components measured at a common location, thus minimizing phone line or facsimile data transmission, so this configuration should not be ruled out.

6. SUMMARY

In this report we have analyzed the potential of a forward-scatter Doppler radar sounding system for measurement of winds up to heights of about 15 km. Because of the large scattering volume intercepted by the transmitter and receiver beams, the system averages spatially over a fairly large horizontal area, but is capable of measuring the winds continually in real time. For many weather service applications, the spatially averaged wind has more meaning than a point measurement because of the scales of the synoptic features of interest. However, present technology offers no immediate promise of providing temperature and humidity data aloft except by balloon sounding.

We have considered cost and feasibility aspects of the system in only a very preliminary way in this report. The next step should be twofold.

(1) An experimental program should begin to establish the maximum scattering angles that can be used with new processing and modulation techniques. In this report we have proposed a pseudo-random modulation system, but we have recently been able to process for Doppler information using an FM-CW radar. These systems should be compared as potential candidates and should be used to collect data in various seasons and climates to determine percent of outage time vs. altitude.

(2) A much more complete cost and configuration analysis should be carried out in conjunction with the NWS. Very important considerations would be whether many of the weather radar sites and personnel could be utilized in the wind sounding system, and whether fewer and very much cheaper radiosonde systems could be used if winds could be measured independent of the balloon system.

7. REFERENCES

Atlas, D. (1969), The measurement of crosswind by non-coherent dual-arm bistatic radio tropo-scatter techniques, *J. Atmos. Sci.* 26:1122-1127.

Atlas, D., K. Naito, and R.E. Carbone (1968), Bistatic microwave probing of a refractively perturbed clear atmosphere, *J. Atmos. Sci.* 25: 257-268.

Bailey, C.C. (1972), Dispersion properties of troposcatter channels, presented at Natl. Telecommunications Conf., Houston, Dec. 1972.

Barrow, B.B., L.G. Abraham, W.M. Cowan, Jr., and R.M. Gallant (1969), Indirect atmospheric measurements utilizing Rake tropospheric scatter techniques, Pt. I: The Rake tropospheric scatter technique, *Proc. IEEE* 57:537-551.

Birkemeier, W.P., H.S. Merrill, Jr., D.H. Sargeant, D.W. Thomson, C.M. Beamer, and G.T. Bergemann (1968), Observation of wind-produced Doppler shifts in tropospheric scatter propagation, *Radio Sci.* 3: 309-317.

Birkemeier, W.P., P.F. Duvoisin, A.B. Fontaine, and D.W. Thomson (1969), Indirect atmospheric measurements utilizing Rake tropospheric scatter techniques, Pt. II: Radiometeorological interpretation of Rake channel-sounding observations, *Proc. IEEE* 57:552-559.

Booker, H.G., and W. Gordon (1950), A theory of radio scattering in the troposphere, *Proc. IRE* 38:401-412.

Booker, H.G., and J.T. deBettencourt (1955), Theory of radio transmission by tropospheric scattering using very narrow beams, *Proc. IRE* 43: 281-290.

Cooper, G.R., and C.D. McGillem (1971), *Probabilistic Methods in Signal and System Analysis*, Holt, Rinehart and Winston, New York.

Cox, D.C. (1972), Delay-Doppler characteristics of multipath propagation at 910 MHz in a suburban mobile radio environment, *IEEE Trans.* AP-20:625-635.

Doviak, R. J., J. Goldhirsh, and A. R. Miller (1972), Bistatic-radar detection of high-altitude clear-air atmospheric targets, *Radio Sci.* 7:993-1004.

Farnett E.C., T.B. Howard, and G.H. Stevens (1970), Pulse-compression radar, Ch. 20 of *Radar Handbook*, M.I. Skolnik, ed., McGraw-Hill, New York.

Lammers, U.H.W., and R.L. Olsen (1973), Bistatic measurement of meteorological and propagation parameters with a high-resolution Ku-band scatter system, in *Proc. Intl. IEEE/G-AP Symp., Boulder, Colo., Aug. 21-24, 1973*, IEEE, New York, 200-203

Monsen, P. (1972), Performance of an experimental angle-diversity troposcatter system, *IEEE Trans.* COM-20: 242.

Nathanson, F.E. (1969), *Radar Design Principles*, McGraw-Hill, New York.

Ottersten, H. (1969), Radar backscattering from the turbulent clear atmosphere, *Radio Sci.* 4:1251-1255.

Richter, J.H. (1969), High resolution tropospheric radar sounding, *Radio Sci.* 4:1261-1268.

Villars, F., and V.F. Weisskopf (1955), On the scattering of radio waves by turbulent fluctuations of the atmosphere, *Proc. IRE* 43:1232-1239.

APPENDIX

RANDOM AND PSEUDO-NOISE MODULATION SYSTEMS

A. RANDOM-CODED WAVEFORMS

In deciding what type of digital signal to use to phase-modulate the carrier of the r-f sounding signal, keep in mind that, within reasonable limits, the estimated complex response should not depend on the sounding signal. The modulating signal should be wideband and have a narrow autocorrelation function. Imagine that the signal is designed by flipping a coin and assigning the value of +1 for a head and -1 for a tail. To be more precise, assume a sequence of independent Bernoulli trials having outcome +1 with probability one-half and outcome -1 with probability one-half. Let a(t) be a binary random waveform obtained by assigning the current value at t and assigning the next value every τ_1 sec. This random waveform is used to phase-modulate an r-f carrier to derive a real sounding waveform of the form

$$x(t) = \cos\left[\omega t + \frac{a(t) - 1}{2}\pi + \theta\right] , \qquad (A1)$$

where amplitude has been taken as unity without loss of generality, and θ is an arbitrary phase angle. This sounding signal is more conveniently written in terms of its complex envelope, Env x(t). Thus from (A1) we write

$$\text{Env } x(t) = e^{j\left[\frac{a(t) - 1}{2}\right]\pi + \theta} . \qquad (A2)$$

But this is the same as

$$\text{Env } x(t) = a(t)\, e^{j\theta} . \qquad (A3)$$

The correlator receiver correlates the received waveform with a delayed replica of the transmitted waveform and it is easy to design the receiver so that the output is the complex envelope (in quadrature form) of the cross correlation function. Neglect, for the moment, that the random sequence must be available at the receiver to perform the correlation. Also assume that the path is perfect, i.e., the transmitted waveform is simply delayed in time by T, and attenuated to produce the re-received waveform. Thus the real received waveform will have amplitude B, where B is the real attenuation of the path. Also a phase term (possibly time varying) dependent on exact path length will be introduced into the complex envelope of the received signal. It is this time-varying phase term that contains Doppler information on the cross-wind velocity.

This phase term is denoted by ϕ while the complex envelope of the received signal y(t) is given by

$$\text{Env } y(t) = \text{Env } B\, x(t-T) = Ba(t-T)\, e^{j\theta + j\phi} . \qquad \text{(A4)}$$

It is relatively easy to instrument a correlation receiver to obtain the complex envelope of the cross-correlation between the received waveform and a replica of the transmitted waveform which has been delayed by T'. The output, following a low pass filter, is actually two voltages, sometimes called the in-phase and quadrature components; these two voltages are the real and imaginary parts of the complex envelope of the cross-correlation function. If this complex envelope is denoted by u(t), the receiver output is

$$u(t) = \text{Env}\left[E\left\{ x(t-T')\, y(t) \right\} \right] = \frac{1}{2} E\left\{ \text{Env } x(t-T')\, \text{Env}^* \, y(t) \right\} \qquad \text{(A5)}$$

where $E\{\cdot\}$ is an expectation over the random sequence. The reference signal into the correlator has a phase angle ϕ' so that the receiver output is

$$u(t) = \frac{B}{2} E\left\{ a(t-t')\, a(t-T) \right\} e^{j(\phi'-\phi)} . \qquad \text{(A6)}$$

The expected value is the autocorrelation function of a(t), so that the output can be rewritten as

$$u(t) = \frac{B}{2} R_a(\tau)\, e^{j(\phi'-\phi)} \qquad \text{(A7)}$$

where $\tau = T - T'$, the difference in delay between the received waveform and the reference waveform. Since ϕ is generally time-varying, it is clear that a spectral analysis of u(t) yields the desired Doppler information on cross-path wind velocities. The reference signal delay can be changed with time which is reflected in the fact that the output is a function of time.

It is clear from (A7) that it is desirable to know certain statistical properties of random binary sequences. Of the three properties of interest stated in the next section, the important property here is that the autocorrelation function vanishes for shifts beyond one segment length. If there are N elements in a binary random sequence and if these elements are generated τ_1 sec apart, the autocorrelation function is as shown in figure A1.

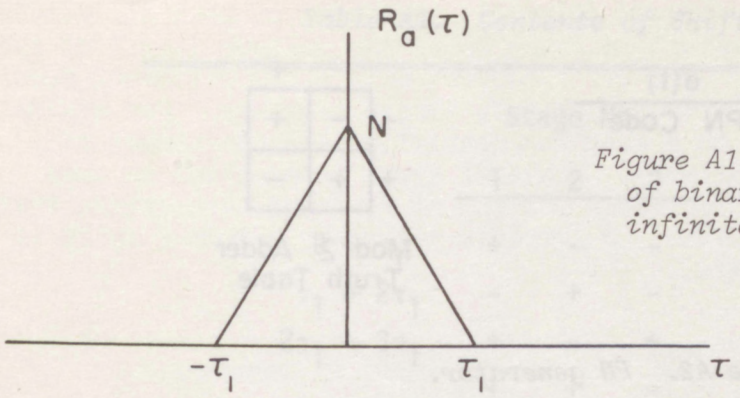

Figure A1. Autocorrelation function of binary waveform generated from infinite length random sequence.

For a general case, each path will produce a complex term such as (A7) in the output; added together, these terms produce the output complex envelope. It is clear that to improve the resolution of the sounder, τ_1 must be decreased, i.e., the coin must be flipped faster. Note that this is the same as increasing the bandwidth of the sounding signal and it is well know (e.g., Cooper and McGillem, 1971), that if a random sounding signal has a bandwidth that is much greater than the channel, the impulse response of the channel is equal to the cross-correlation between the received signal and a delayed replica of the sounding signal. This means that if τ_1 is small enough, the complex envelope of the output of the correlator receiver is a good approximation to the complex envelope of the impulse response of the channel, so that the sounder will produce range bins; spectral analyses of the signals from these range bins will produce Doppler information.

B. PSEUDO-NOISE WAVEFORMS

In the previous section, a sounder was described that used a random sequence to phase-modulate an r-f carrier. Since a correlation receiver is used, it is necessary to have the same random sequence available at the receiver, which is not generally possible. However, (A7) shows that the correlation property of the sequence is actually what is measured so that a deterministic waveform with desirable correlation properties would work well as a random sequence. There are a number of such deterministic waveforms, e.g., Barker codes, polyphase codes, and Huffman sequences, but perhaps the easiest to generate are the pseudo-noise codes or sequences. These pseudo-noise codes are so called because they have the properties of noise but are completely deterministic and periodic. Other names applied to these codes are pseudo-random codes, shift-register sequences, PN codes, maximal length sequences or m sequences. Here they are called PN (for pseudo-noise) sequences while the device that generates them is called a PN generator.

Before considering the general properties of the PN sequence, it is instructive to consider a simple example. A PN generator that

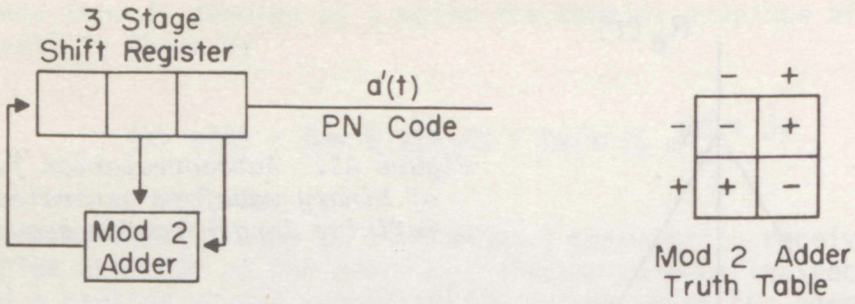

Figure A2. PN generator.

generates a short PN sequence is shown in figure A2. There are only two components, a three-stage shift register and a modulo 2 adder that uses carry-free arithmetic. The shift register is clocked every τ_1 sec and produces a sequence element every τ_1 sec. The outputs of the second and third stage of the shift register are added modulo 2 and the carry-free output is taken to the first stage of the shift register. Assume that the shift register starts with all minus 1's in the three registers. In this case the output of the mod 2 adder is also minus 1, and the PN generator would put out an endless string of minus 1's. Since an endless string of minuses does not have the desired correlation properties, the PN generator is not allowed to start with all minuses. Other than the requirement that there be at least one positive stage in the shift register, the starting point can be anything. Assume that the first stage is a plus and stages 2 and 3 are minus. Then the contents of the register at each shift are as shown in Table A1.

The output signal is simply a time picture of the contents of the last stage of the shift register. To obtain the desired correlation properties of PN codes, it is necessary that the code be continued in time, i.e., truncation of the code will affect the correlation function. The PN waveform a'(t), which can be used to phase-modulate the sounding signal, is shown in figure A3.

The PN codes are used extensively in communication for spread spectrum modulation, for secure communication systems, and for code division multiple access. They have been well studied and are well understood (Farnett et al., 1970; Nathanson, 1969). However, to derive their properties requires that they be characterized mathematically by binary polynomials. The properties of these polynomials then determine the properties of the codes that they represent. Since the purpose here is to gain an intuitive grasp of the PN sequences, the pertinent properties of the sequences are simply stated.

The first important property is the length of the sequence before it repeats. For an n-stage shift register, the possible number of different combinations of plus and minus in the register is 2^n, but the

Table A1. Contents of Shift Register

	Stage No. 1	2	3	
$0 \rightarrow \tau_1$	+	-	-	
$\tau_1 \rightarrow 2\tau_1$	-	+	-	
$2\tau_1 \rightarrow 3\tau_1$	+	-	+	
	+	+	-	Identical Points
	+	+	+	
	-	+	+	
	-	-	+	
$7\tau_1 \rightarrow 8\tau_1$	+	-	-	
.	.	.	.	
.	.	.	.	
.	.	.	.	

repeats output sequence

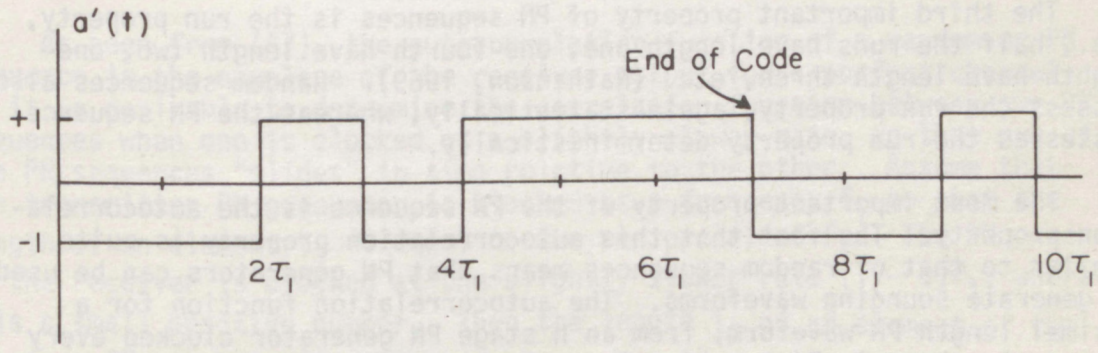

Figure A3. PN Waveform.

all-minus condition is not allowed (since it continues to generate minuses only), so the number of combinations, and hence the maximum length of the sequence before it repeats, is 2^n-1. However, only a few different feedback connections will result in the maximal length sequence. For maximal length the last stage must be a feedback connection and the number of feedback connections must be even. Table A2 gives information on some different PN sequences and for each, one set of feedback connections that gives a maximal length sequence. A complete table for n from 2 to 20 is given by Farnett et al. (1970).

Table A2. Information on Maximal Length PN Sequences.

Number of Stages	Maximal Length	Number of Maximal Length Sequences	Feedback Connections
2	3	1	2,1
3	7	2	3,2
4	15	2	4,3
5	31	6	5,3
9	511	48	9,5
10	1,023	60	10,7
15	32,767	1,800	15,14
20	1,048,575	24,000	20,17

The second important property of PN sequences is the balance property that the total of 1's is approximately (i.e., $\pm$ 1) the number of zeros. Random sequences obtained by flipping a coin also possess the balance property. However, each PN sequence is deterministically rather than statistically balanced.

The third important property of PN sequences is the run property, i.e., half the runs have length one, one-fourth have length two, one-eighth have length three, etc. (Nathanson, 1969). Random sequences also possess the run property, again statistically, whereas the PN sequence possesses the run property deterministically.

The most important property of the PN sequence is the autocorrelation property. The fact that this autocorrelation property is quite similar to that of random sequences means that PN generators can be used to generate sounding waveforms. The autocorrelation function for a maximal length PN waveform, from an n stage PN generator clocked every τ_1 sec, is shown in Figure A4. The only two differences between this autocorrelation function and that of Figure A1 are the peaks caused by periodicity and the value of -1 away from the peaks. However, the effects

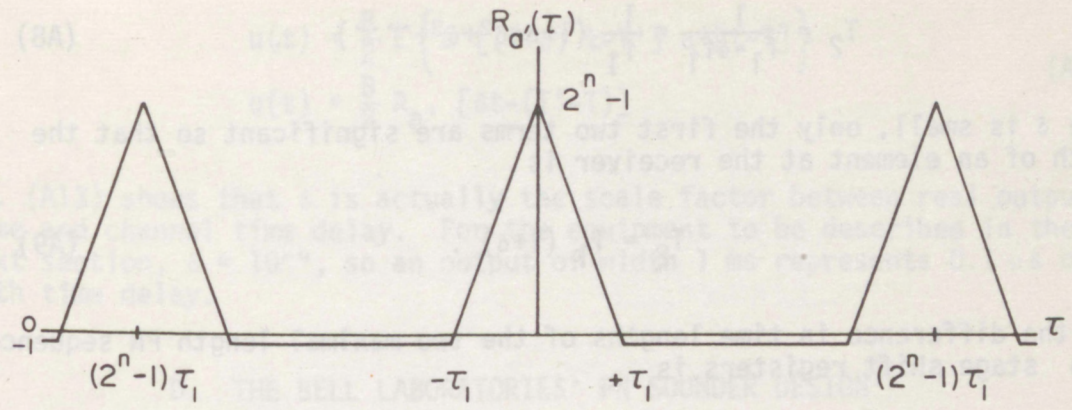

Figure A4. Autocorrelation functon for maximal length PN waveform from n-stage shift register.

of these differences will be negligibly small since $2^n - 1$ grows very rapidly as n increases. So for moderate sized shift registers, the PN sequence can, for practical channel sounding purposes, be considered a random sequence. Thus the sounder described in the previous section becomes a very worthwhile device when PN generators are used to modulate the sounding waveform.

C. TIME DELAY SCANNING

In the previous section there was no provision to change the relative delay between the two sequences. This means that the sounder would continually measure the wind at only one delay (or equivalently one height); this delay would be the relative delay between the two sequences. A method of scanning this relative delay is to clock one of the PN generators at a slightly slower rate than the other. Then one of the PN sequences "slides" in time relative to the other PN sequence and the output of a correlator is the entire correlation function.

As seen from (A7), the autocorrelation function of a random or PN sequence is the envelope of the receiver output for a perfect channel. So it is desirable to determine the correlation function between two PN sequences when one is clocked at a slightly slower rate, so that one of the PN sequences "slides" in time relative to the other. Assume that the transmitter PN generator is clocked at a frequency f_1 so that the length of an element T_1 is equal to the reciprocal of f_1. The PN generator at the receiver is clocked at the slightly slower rate $(1 - \delta)f_1$, where δ is a small positive number. Then the length T_2 of an element of the receiver PN sequence is

$$T_2 = \frac{1}{f_1 - \delta f_1} = \frac{1}{f_1}\,(1+\delta+\delta^2+\delta^3+\cdots\cdots) \quad . \tag{A8}$$

Since δ is small, only the first two terms are significant so that the length of an element at the receiver is

$$T_2 = T_1\,(1+\delta) \quad . \tag{A9}$$

Thus the difference in time lengths of the two maximal length PN sequences for n stage shift registers is

$$\Delta_T = T_1\,\delta(2^n-1) \quad . \tag{A10}$$

For this time difference to have a negligible effect on the correlation function, the largest time offset between elements of the sequence must be much less than the element length. The largest offset occurs in the last element and is given by Δ_T, so this inequality must hold:

$$\Delta_T = T_1\,\delta(2^n-1) \ll T_1 \tag{A11}$$

or equivalently,

$$\delta \ll \frac{1}{(2^n-1)} \quad . \tag{A12}$$

For the equipment described here n = 9 so that the right is approximately 2×10^{-3} and $\delta = 10^{-4}$. Thus the inequality is well satisfied. Cox (1972) points out that with n = 9, correlation function distortion is slight for $\delta = -0.2\times10^{-3}$ and considerable for $\delta = 10^{-3}$.

It is clear from (A9) that the effect of clocking one PN generator at a slower rate is to change the time scale for the PN sequence out of that generator. If the channel is perfect with delay T, the received PN sequence is a'(t-T). Also, the reference PN sequence (which is clocked at a slightly slower rate) is a'[(1-δ) t-T'] where T' is the delay of the reference signal. The envelope of the receiver output is proportional to the autocorrelation function as shown by (A7). The envelope of the receiver output is then

$$u(t) = \frac{B}{2} E\left\{a'[(1+\delta)\ t-T']\ a'[t-T]\right\}$$
$$u(t) = \frac{B}{2} R_{a'}\ [\delta t-(T'-T)] \qquad \text{(A13)}$$

Eq. (A13) shows that δ is actually the scale factor between real output time and channel time delay. For the equipment to be described in the next section, $\delta = 10^{-4}$, so an output of width 1 ms represents 0.1 μs of path time delay.

D. THE BELL LABORATORIES' PN SOUNDER DESIGN

The particular PN wind sounder system described here is based on a communication channel sounder designed at Bell Telephone Laboratories by H. L. Schneider and used there to study and characterize the troposcatter communications channel (Monsen, 1972; Bailey, 1972). A similar sounder was used by Cox (1972) to characterize the mobile radio channel.

A block diagram of the transmitter portion of the sounder is shown in figure A5. The PN generator is driven at a 10-MHz rate by a sine wave derived from a stable clock. The PN generator has a nine-stage shift register; hence the output has length of 511 elements before it repeats. The 70-MHz i-f is also derived from the stable clock and the PN sequence phase modulates the i-f. The transmitted signal is then derived by modulating the i-f signal to r-f by mixing the i-f with a 2100 MHz sine wave which has been derived by multiplication up from the stable 15-MHz clock. This signal then has a center frequency of 2170 MHz. The sounding signal is amplified by a wide-band transistorized r-f amplifier that does not distort the spectrum. For sounding of troposcatter paths, the signal is amplified by a 1 kW klystron amplifier.

A block diagram of the PN sounder receiver is shown in figure A6. The received waveform is mixed down to 70 MHz i-f and then correlated with a PN sequence that has been modulated up to 70 MHz. The integrating filter is a finite time integrator with integration time approximately 51.1 μs, the length of the PN sequence. The receiver is a quadrature receiver so the outputs of the finite time integrators are the real and imaginary parts of the complex envelope of the impulse response. The PN generator that is used to derive the reference signal is driven at a rate that is slightly less than the PN generator rate in the transmitter, resulting in a sweeping of delay as described in the previous section. An additional PN generator is driven at the same rate as in the transmitter portion and when the two PN generators in the receiver are offset by a desired amount (2 μs channel time, or 20 ms real time), a logic section resets the reference signal PN generator to the same point as the PN generator that is being driven at 10 MHz. The outputs are the real and imaginary parts of the complex impulse response;

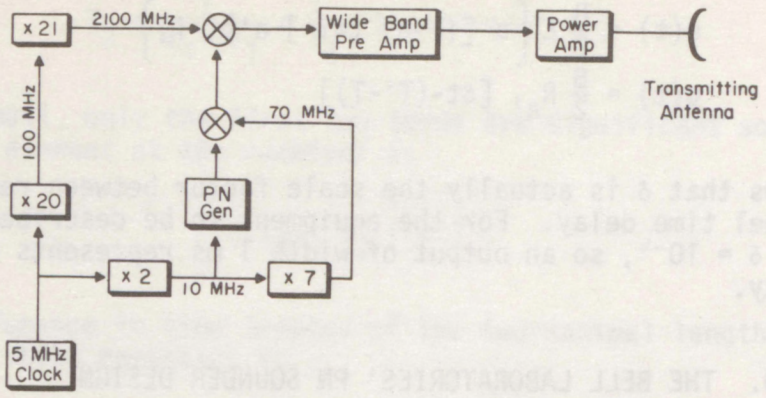

Figure A5. Transmitter for PN channel sounder.

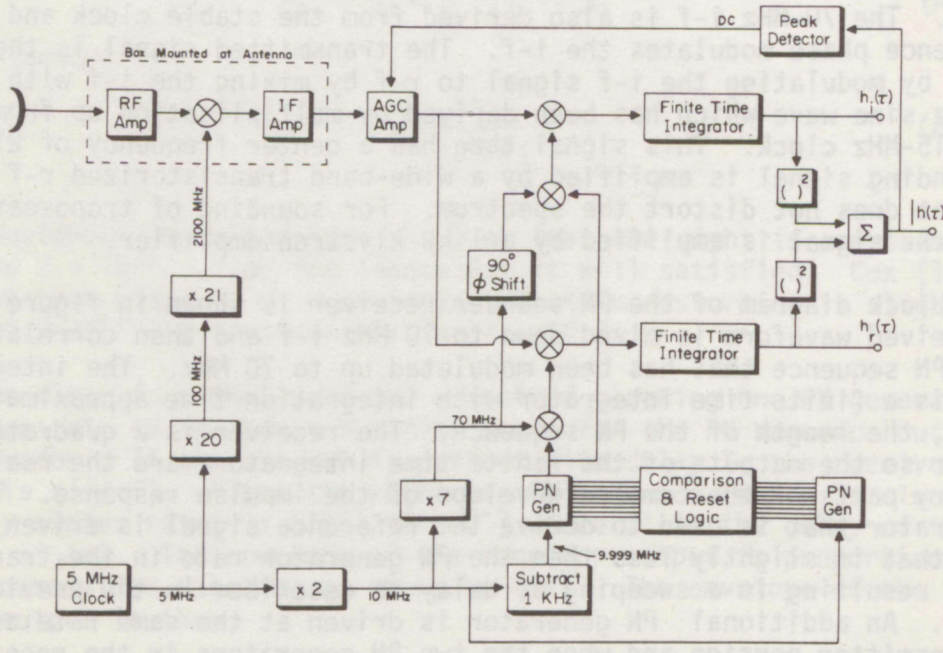

Figure A6. Receiver for PN channel sounder.

spectral analysis of this output yields the Doppler information about cross-wind velocities.

In order to estimate the cross-wind velocity, a signal-to-noise ratio somewhat greater than unity is required at the output of the receiver. One of the distinct advantages of a PN sounder (as opposed to a sounder with analog modulation) is that it is quite easy to approach closely the optimum receiver because the digitally modulated signal can be accurately reproduced at a remote station.

The optimum receiver, whether a matched filter or equivalent correlator, has a peak signal power to average noise power output ratio SNR_o, for one pass through the code, of

$$SNR_o = \frac{2E_s}{N_o} \tag{A14}$$

where E_s is the received signal energy coherently integrated in one code word and $N_o/2$ is the two-sided noise power spectral density. The coherent integration is over the length of the finite time integrator which is equal to the code length, so that if P_s is the received signal power averaged over the coherent integration time T,

$$E_s = T P_s \tag{A15}$$

Noting that the average input noise power is $P_n = N_o B$ where B is the bandwidth of the receiver, the output peak signal-to-noise ratio is

$$E_s = 2TB \frac{P_s}{P_n} \tag{A16}$$

or the optimum receiver has a processing gain of 2TB. This result is valid for any signal, showing immediately the problem that arises if the cross-wind velocity is measured directly by transmitting a short r-f pulse, since the bandwidth is then approximately the reciprocal of the integration time. Hence, the output peak signal-to-noise ratio is only twice the input average signal-to-noise ratio and the doubling simply represents the fact that the output ratio is a peak signal-to-noise ratio. For an ideal PN sounder, the bandwidth is approximately the reciprocal of the element length and the coherent integration time is the sequence length times the element length so that the processing gain is twice the number of code elements, $2(2^n - 1)$ which is 1022 or 30 dB. For practical PN sounders this result is degraded only a few dB (Nathanson, 1969).

☆U.S. GOVERNMENT PRINTING OFFICE: 1975—677-347/1205 REGION NO. 8

ENVIRONMENTAL RESEARCH LABORATORIES

The mission of the Environmental Reasearch Laboratories is to study the oceans, inland waters, the lower and upper atmosphere, the space environment, and the earth, in search of the understanding needed to provide more useful services in improving man's prospects for survival as influenced by the physical environment. Laboratories contributing to these studies are:

Atlantic Oceanographic and Meteorological Laboratories (AOML): Geology and geophysics of ocean basins and borders, oceanic processes, sea-air interactions and remote sensing of ocean processes and characteristics (Miami, Florida).

Pacific Marine Environmental Laboratory (PMEL): Environmental processes with emphasis on monitoring and predicting the effects of man's activities on estuarine, coastal, and near-shore marine processes (Seattle, Washington).

Great Lakes Environmental Research Laboratory (GLERL): Physical, chemical, and biological, limnology, lake-air interactions, lake hydrology, lake level forecasting, and lake ice studies (Ann Arbor, Michigan).

Atmospheric Physics and Chemistry Laboratory (APCL): Processes of cloud and preciptation physics; chemical composition and nucleating substances in the lower atmosphere; and laboratory and field experiments toward developing feasible methods of weather modification.

Air Resources Laboratories (ARL): Diffusion, transport, and dissipation of atmospheric contaminants; development of methods for prediction and control of atmospheric pollution; geophysical monitoring for climatic change (Silver Spring, Maryland).

Geophysical Fluid Dynamics Laboratory (GFDL): Dynamics and physics of geophysical fluid systems; development of a theoretical basis, through mathematical modeling and computer simulation, for the behavior and properties of the atmosphere and the oceans (Princeton, New Jersey).

National Severe Storms Laboratory (NSSL): Tornadoes, squall lines, thunderstorms, and other severe local convective phenomena directed toward improved methods of prediction and detection (Norman, Oklahoma).

Space Environment Laboratory (SEL): Solar-terrestrial physics, service and technique development in the areas of environmental monitoring and forecasting.

Aeronomy Laboratory (AL): Theoretical, laboratory, rocket, and satellite studies of the physical and chemical processes controlling the ionosphere and exosphere of the earth and other planets, and of the dynamics of their interactions with high-altitude meteorology.

Wave Propagation Laboratory (WPL): Development of new methods for remote sensing of the geophysical environment with special emphasis on optical, microwave and acoustic sensing systems.

Marine EcoSystem Analysis Program Office (MESA): Plans and directs interdisciplinary analyses of the physical, chemical, geological, and biological characteristics of selected coastal regions to assess the potential effects of ocean dumping, municipal and industrial waste discharges, oil pollution, or other activity which may have environmental impact.

Weather Modification Program Office (WMPO): Plans and directs ERL weather modification research activities in precipitation enhancement and severe storms mitigation and operates ERL's research aircraft.

NATIONAL OCEANIC AND ATMOSPHERIC ADMINISTRATION
BOULDER, COLORADO 80302